6090 *J. Phys. Chem. A* **2008,** *112,* 6090–6097

Unimolecular Elimination of HF and HCl from Chemically Activated $CF_3CFClCH_2Cl$

Oksana Zaluzhna,[†] Jay G. Simmons, Jr.,[†] George L. Heard,[†] D. W. Setser,[†,‡] and Bert E. Holmes*[,†]

Department of Chemistry, University of North Carolina—Asheville, One University Heights, Asheville, North Carolina 28804-8511, and Department of Chemistry, Kansas State University, Manhattan, Kansas 66506

Received: January 17, 2008; Revised Manuscript Received: March 25, 2008

The unimolecular reactions of $CF_3CFClCH_2Cl$ molecules formed with 87 kcal mol^{-1} of vibrational energy by recombination of CF_3CFCl and CH_2Cl radicals at room temperature have been characterized by the chemical activation technique. The 2,3-ClH and 2,3-FH elimination reactions, which have rate constants of $(2.5 \pm 0.8) \times 10^4$ and $(0.38 \pm 0.11) \times 10^4$ s^{-1}, respectively, are the major reactions. The 2,3-FCl interchange reaction was not observed. The *trans* (or *E*)-isomers of $CF_3CF{=}CHCl$ and $CF_3CCl{=}CHCl$ are favored over the *cis* (or *Z*)-isomers. Density functional theory at the B3PW91/6-31G(d′,p′) level was used to evaluate thermochemistry and structures of the molecule and transition states. This information was used to calculate statistical rate constants. Matching the calculated to the experimental rate constants for the *trans*-isomers gave threshold energies of 62 and 63 kcal mol^{-1} for HCl and HF elimination, respectively. The threshold energy for FCl interchange must be 3−4 kcal mol^{-1} higher than for HF elimination. The results for $CF_3CFClCH_2Cl$ are compared to those from $CF_3CFClCH_3$; the remarkable reduction in rate constants for HCl and HF elimination upon substitution of one Cl atom for one H atom is a consequence of both a lower $\langle E \rangle$ and higher threshold energies for $CF_3CFClCH_2Cl$.

I. Introduction

A recent objective of our studies of unimolecular reactions of haloalkanes by the chemical activation technique has been to characterize the interchange reaction of F and Cl atoms located on adjacent carbons.[1–4] The best examples have been $CF_2ClCHFCH_3$,[2] $CF_2ClCF_2CH_3$[3,4] and $CF_2ClCHFC_2H_5$.[1] The existence of Br−F interchange also has been demonstrated for $CF_2BrCF_2CH_3$,[5] and Cl−F interchange exists for several fluorochloroethanes.[6–8] In the present study we have extended the program to $CF_3CFClCH_2Cl$ in anticipation that 2,3-FCl or 1,2-FCl interchange might be observed in competition with 2,3-ClH and 2,3-FH elimination. In fact, neither $CF_3CCl_2CH_2F$ nor $CF_2ClCF_2CH_2Cl$ was observed, largely because of unfavorable thermochemistry, and HCl and HF elimination are the preferred decomposition pathways for $CF_3CFClCH_2Cl$ rather than FCl interchange. These pathways can be compared to the fully characterized HCl (DCl) and HF (DF) elimination reactions[10] of $CF_3CFClCH_3$-d_0, -d_1, -d_2, -d_3; the replacement of a H-atom by a Cl-atom in the 3-position greatly reduces the rate constant for HX (X = Cl, F) elimination and understanding this trend will be the main point of this paper. In future work, we will describe the $CF_2ClCFClCH_2F$ and $CF_2ClCF_2CH_2Cl$ systems, which do exhibit Cl−F interchange reactions.

The vibrationally excited $CF_3CFClCH_2Cl$ molecules were generated by the recombination of CF_3CFCl and CH_2Cl radicals, which were obtained from photolysis of CF_3CFClI and CH_2ClI. The expected decomposition products, D_i, are in eqs 1 and 2 and the collisional stabilization product, S, is in eq 3.

$$CF_3CFClCH_2Cl^* \rightarrow CF_3CF{=}CHCl\ (E \text{ and } Z \text{ isomers}) + HCl \quad (1)$$

$$\rightarrow CF_3CCl{=}CHCl\ (E \text{ and } Z \text{ isomers}) + HF \quad (2)$$

$$\rightarrow CF_3CFClCH_2Cl + M \quad (3)$$

Collisional deactivation can be safely assumed to be efficient in these systems,[9–12] and the product ratio, D_i/S, equals the rate ratio, $k_i[CF_3CFClCH_2Cl^*]/k_M[M][CF_3CFClCH_2Cl^*]$, which is a linear equation when D_i/S is plotted versus inverse pressure, [M]. The plot has a slope of k_i/k_M and an intercept of zero. The experimental rate constants for HX elimination were determined from the plots of D_i/S versus the inverse pressure.

The *E* isomer (which has the F and Cl or the two Cl atoms in the *trans*-position) is the favored isomer. For simplicity we will refer to the *E*-isomer as the *trans*-isomer and the *Z*-isomer as the *cis*-isomer. The symmetric radical recombination products, $C_2H_4Cl_2$ and $(CF_3CFCl)_2$, were observed, but not studied. Disproportionation reactions are of minor importance for the CF_3CFCl and the CH_2Cl radicals.

Assuming that the calculated structures of the transition states are reliable, the remaining variables in the computation of rate constants are the threshold energies for reaction, E_0, and the average energy of the $CF_3CFClCH_2Cl$ molecules, $\langle E \rangle$. The latter are determined by the $CH_2Cl{-}CFClCF_3$ bond dissociation energy. Based upon several isodesmic reactions to be presented, this bond energy is ≈5 kcal mol^{-1} lower than $CH_3{-}CFClCF_3$, and the average energy of the $CF_3CFClCH_2Cl$ molecules is 87 ± 3 kcal mol^{-1}. The apparent reduction in the carbon−carbon bond energy for molecules with adjacent chlorine or adjacent fluorine and chlorine atoms is a question that needs further study.[13]

[†] University of North Carolina—Asheville.

[‡] Kansas State University.

10.1021/jp800488q CCC: $40.75

Threshold energies were assigned to k_{HCl} and k_{HF} and a lower limit was estimated for the threshold energy of the Cl−F interchange by matching experimental rate constants to statistical RRKM rate constants. In the rate constant calculations, the CH_2Cl and CF_3 internal rotations were treated as symmetric rotors with a single barrier height and an average reduced moment. The vibrational frequencies and moments of inertia were obtained from density functional theory (DFT) using the B3PW91/6-31G(d′,p′) method, just as for $CF_3CFClCH_3$.[10] Because the natures of the HF and HCl transition states were discussed together with the primary and secondary isotope effects in the study[10] of $CF_3CFClCH_3$-d_0, -d_1, -d_2, -d_3, we will focus attention in this work on how substitution of a Cl atom for a H atom in the CH_3 group affects the HCl and HF elimination channels.

II. Experimental Methods

The experiments for the $CF_3CFClCH_2Cl$ system were done in the same manner as those previously described for $CF_3CFClCH_3$, except that CH_3I was replaced with CH_2ClI. The only major difference was the need to use larger photolysis vessels to achieve lower pressures for the $CF_3CFClCH_2Cl$ system. Data were collected for a pressure range of 0.05−0.002 Torr. The CF_3CFClI and CH_2ClI were purchased from SynQuest Chemicals and Aldrich, respectively, and used without purification, except for several freeze−thaw pump cycles when loading samples on the vacuum line. The samples to be photolyzed for kinetic analyses were prepared by measuring 1.55−1.60 Torr of each iodide in a 4.26 cm^3 calibrated vessel with subsequent transfer to Pyrex reaction vessels ranging is size from 0.60 to 5.0 L. The pressure in the reaction vessel was determined by adding together the pressure of the iodides determined from the ideal gas law and any residual pressure in the vessel, before transfer of the CF_2CFClI and CH_2ClI samples. Pressures were measured using an MKS 270 electronic manometer. Depending on the vessel volume, photolysis times were between 10−30 min using an Oriel 200-W mercury lamp. A few samples were photolyzed using an Oriel 68811 500-W Xe/Hg lamp, but the results were indistinguishable from data obtained with the 200-W Hg lamp. Experiments to identify the photolysis products typically had 3−4 μmol of each iodide and were photolyzed 4−5 times longer than for experiments which were used to measure D_i/S ratios. All samples were prepared in glass, high-vacuum lines.

Products were identified by mass spectral analysis of reaction mixtures separated by a Shimadzu Gas Chromatograph-17A containing a 60 m by 0.25 mm Rtx-VMS capillary column and a Shimadzu Gas Chromatograph−Mass Spectrometer QP-5000. Commercial samples were available for CH_2ClI, CF_3CFClI, and $CF_3CCl{=}CHCl$ (SynQuest). Photolysis of CH_2ClI and CF_3CFClI at high pressure provided a high yield of $CF_3CFClCH_2Cl$, and it was identified by the mass spectral data given in Table 1.

The identity of *E*- and *Z*-$CF_3CF{=}CHCl$ was established by analysis of products from two synthetic methods (X = H or Cl) using reactions 4 and 5.

$$\cdot CF_3 + CXF{=}CHCl \rightarrow CF_3CXFCHCl\cdot \tag{4}$$

$$\cdot CF_3 + CF_3CXFCHCl\cdot \rightarrow XCF_3 + E\text{- and } Z\text{-}CF_3CF{=}CHCl \tag{5}$$

TABLE 1: Mass Spectral Fragmentation Data at 70 eV (*m/e*, Relative Abundance (RA), and Assignment)

m/e	RA	assignment
$CF_3CFClCH_2Cl$		
115	100	$C_2Cl_2FH_2^+$
117	63.5	$C_2F_3H^{35}Cl^+$, $C_2{}^{35}Cl^{37}ClFH_2^+$
49	55.5	$C^{35}ClH_2^+$
69	43.8	CF_3^+
51	37.5	CF_2H^+
trans-$CF_3CF{=}CHCl$		
69	100	CF_3^+
113	92	$C_3F_4H^+$
98	80	$C_2F_2H^{35}Cl^+$
148	68	$C_3F_4H^{35}Cl^+$
31	49	CF^+
129	29	$C_3F_3H^{35}Cl^+$
150	22	$C_3F_4H^{37}Cl^+$
cis-$CF_3CF{=}CHCl$		
69	100	CF_3^+
113	74	$C_3F_4H^+$
98	71	$C_2F_2H^{35}Cl^+$
148	55	$C_3F_4H^{35}Cl^+$
31	47.6	CF^+
100	22	$C_2F_4^+$
150	17	$C_3F_4H^{37}Cl^+$
trans-$CF_3CCl{=}CHCl$		
129	100	$C_3F_3H^{35}Cl^+$
164	42	$C_3F_3H^{35}Cl_2^+$
69	41	CF_3^+
131	32	$C_3F_3H^{37}Cl^+$
166	27	$C_3F_3H^{37}Cl^{35}Cl^+$
cis-$CF_3CCl{=}CHCl$		
129	100	$C_3F_3H^{35}Cl^+$
164	44	$C_3F_3H^{35}Cl_2^+$
69	39	CF_3^+
131	32	$C_3F_3H^{37}Cl^+$
166	26	$C_3F_3H^{37}Cl^{35}Cl^+$
$CF_3CFClCD_2Cl$		
117	100	$C_2{}^{35}Cl_2FD_2^+$
119	64.5	$C_2F_3D_2{}^{35}Cl^+$
51	64	$CD_2{}^{35}Cl^+$
69	60	CF_3^+
85	29	$CF_2{}^{35}Cl^+$
cis- and *trans*-$CF_3CCl{=}CDCl$[a]		
130	100	$C_3F_3D^{35}Cl^+$
69	81	CF_3^+
165	27	$C_3F_3D^{35}Cl_2^+$
167	25	$C_3F_3D^{37}Cl_2^+$
cis- and *trans*-$CF_3CF{=}CDCl$[a]		
69	100	CF_3^+
99	59	$C_2F_2D^{35}Cl^+$
114	55	$C_3F_4D^+$
130	27	$C_3F_3D^{35}Cl^+$

[a] The *cis*- and *trans*-isomers were combined because the RA were similar.

In the first synthesis (X = H), hexafluoroacetone and $CHF{=}CHCl$ were photolyzed 20−30 min using reactant ratios from 1:1 to 5:3, respectively. A small amount of product with retention times of 7.2−7.3 min had the same mass spectrum and retention time as two $CF_3CF{=}CHCl$ products observed in the kinetic runs when samples of CH_2ClI and CF_3CFClI were photolyzed. The presence of *m/e* = 148 and 150 and also 113 with similar relative abundances was evidence for the $CF_3CF{=}CHCl$ geometric isomers. The 148 and 150 mass peaks are the parent ion of *trans*- and *cis*-$CF_3CF{=}CHCl$ (with the two common chlorine isotopes, Cl-35 and Cl-37) and the *m/e* = 113 corresponds to loss of Cl from the parent ions. The second synthesis (X = Cl) involved photolysis of a 5:1 ratio of hexafluoroacetone and $CFCl{=}CHCl$ for 20 min in quartz vessels. The yield was much larger than for the first method and two products were identified with the same mass spectrum and retention times as noted above. As a further test that the assignment was correct for

$CF_3CFClCH_2Cl$ and *trans*- and *cis*-$CF_3CF{=}CHCl$, $CF_3CFClCD_2Cl$ was prepared by photolysis of CD_2ClI and CF_3CFClI. The mass spectra for the deuterium isotopes are in Table 1; the *trans*- and *cis*-isomers of $CF_3CF{=}CDCl$ and $CF_3CCl{=}CDF$ have similar MS fragmentation patterns, thus an average is shown in Table 1.

The assignment of *trans*- versus *cis*-isomers for $CF_3CF{=}CHCl$ (and for $CF_3CCl{=}CHCl$) was made by assuming that the larger yield in all three types of experiments (kinetic runs and the two disproportionation methods) corresponded to the more stable isomer. Electronic structure calculations using DFT with the B3PW91 method and the 6-311+G(2d,p) basis set showed that the *trans*-isomer was 4 kcal mol^{-1} lower in energy than the *cis*-isomer. The $CF_3CCl{=}CHCl$ products were identified using the commercial sample.

The data for the D/S vs $1/P$ plots were obtained with a Shimadzu CG-14A equipped with flame ionization detector (FID) and 0.53 mm by 105 m MXT-624 column. The temperature program for both the FID and MS instruments began with a temperature of 35 °C for 20 min, followed by heating at a rate of 6 °C/min to a maximum temperature of 180 °C, which was maintained for 20 min. The retention times in minutes for the FID instrument were approximately as follows: 11.3 (*trans*-$CF_3CF{=}CHCl$), 12.0 (*cis*-$CF_3CF{=}CHCl$), 23.0 (*trans*-$CF_3CCl{=}CHCl$), 26.2 (CF_3CFClI), 27.4 (*cis*-$CF_3CFClCH_2Cl$) and 39.7 for (CH_2ClI). The branching ratios for the *trans*- and *cis*-isomers also were measured using the Shimadzu GC-MS, QP5000; the relative order of elution was the same as for the FID instrument but the retention times were significantly smaller.

Calibration of the response factors are needed for the FID and the MS detectors so that ratios of peak areas can be converted into molar D_i/S ratios. A commercial sample was available only for *trans*- and *cis*-$CF_3CCl{=}CHCl$. Because authentic samples were not available for the other products (*trans*- and *cis*-$CF_3CF{=}CHCl$ were not isolated in the synthesis summarized by reaction 5), compounds with similar structures were used to estimate the response factors of the detectors. For example, the relative response for $CF_3CCl{=}CHCl/CF_3CF{=}CHCl$ was assumed to be the same as for $CF_3CCl{=}CH_2/CF_3CF{=}CH_2$. Samples of the latter pair were available, and based upon this assumption the response factor for $CF_3CCl{=}CHCl/CF_3CF{=}CHCl$ was 2.0 ± 0.2 for the MS detector and 0.847 ± 0.16 for the FID detector. The detector response for $CF_3CCl{=}CHCl/CF_3CFClCH_2Cl$ was assumed to be similar to that of $CF_3CCl{=}CHCl/CF_3CHClCHClF$ because both pairs differ by the loss of HF. A sample of $CF_3CHClCHClF$ was available from Matrix Scientific. Based on five trials from three different mixtures, the relative response of the FID for $CF_3CCl{=}CHCl/CF_3CHClCHClF$ was 1.3 ± 0.2. Thus, the GC-FID calibration factors for $CF_3CF{=}CHCl/CF_3CFClCH_2Cl$ and $CF_3CCl{=}CHCl/CF_3CFClCH_2Cl$ were 1.53 and 1.30, respectively. We assumed that *trans*- and *cis*-isomers had the same response for either the FID or the MS detectors.

III. Experimental Results

Identification of the five important products shown in reactions 1–3 was relatively straightforward. However, the need for much lower pressures to observe significant amounts of decomposition products relative to the $CF_3CFClCH_3$ experiments initially was surprising. The ratios of *E*(*trans*)- and *Z*(*cis*)-$CF_3CF{=}CHCl/CF_3CFClCH_2Cl$ and *E*(*trans*)-$CF_3CCl{=}CHCl/CF_3CFClCH_2Cl$ were measured by GC-FID. With the calibration factors mentioned above, these experimental product ratios were converted to D_i/S vs $1/P$ plots shown in Figure 1. These plots only extend to $S_i/D < 0.5$, and the slopes provide the high pressure experimental rate constants, which are summarized in Table 2. The *trans*-isomers are the most important decomposition products. The rate constants for *trans*-$CF_3CF{=}CHCl$ and *trans*-$CF_3CCl{=}CHCl$ are $(1.5 \pm 0.1) \times 10^{-3}$ and $(0.25 \pm 0.01) \times 10^{-3}$, respectively in Torr units. The linear plots pass through the origin and the correlation coefficients are 0.95. The *cis*-$CF_3CF{=}CHCl$ product also could be measured by FID, and the D_i/S vs $1/P$ plots gave a rate constant value of $(0.44 \pm 0.03) \times 10^{-3}$ Torr, which corresponds to a *trans*/*cis*-$CF_3CF{=}CHCl$ ratio of 3.3. Because these iodide bath gas molecules are efficient in removing vibrational energy,[9,10] the linear D/S plots for less than 50% decomposition are equivalent to the limiting high pressure chemical activation rate constants, which in turn is the average rate constant, $k_{\langle E \rangle}$, for the narrow energy distribution of the formed molecules.

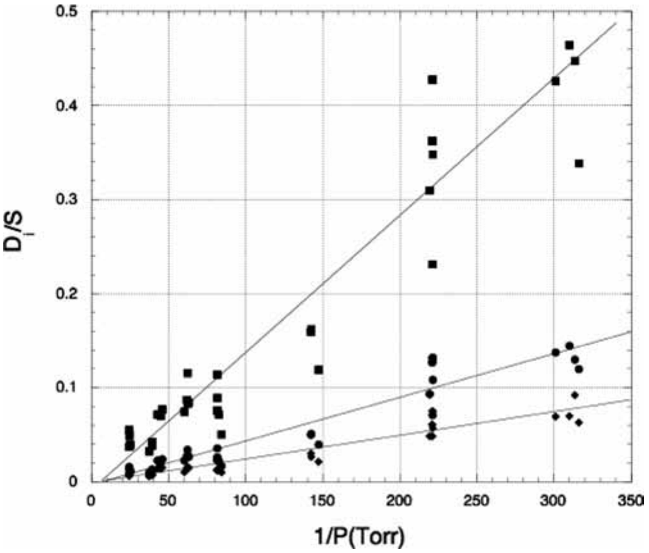

Figure 1. Plots of D_i/S vs pressure^{-1} for $CF_3CFClCH_2Cl$: (■) *trans*-$CF_3CF{=}CHCl/CF_3CFClCH_2Cl$, slope = $(1.46 \pm 0.08) \times 10^{-3}$ Torr, intercept $(-9.4 \pm 12.8) \times 10^{-3}$ with correlation coefficient = 0.95; (●) *cis*-$CF_3CF{=}CHCl/CF_3CFClCH_2Cl$, slope = $(4.4 \pm 0.3) \times 10^{-4}$ Torr, intercept $(-4.2 \pm 4.0) \times 10^{-3}$ with correlation coefficient 0.95; (◆) *trans*-$CF_3CCl{=}CHCl/CF_3CFClCH_2Cl$, slope = $(2.54 \pm 0.14) \times 10^{-4}$ Torr, intercept = $(-1.8 \pm 2.2) \times 10^{-3}$ with correlation coefficient = 0.95. These product ratios were measured by GC/FID.

The yield of *cis*-$CF_3CCl{=}CHCl$ was so small and overlapped with other compounds that the ratio of *trans*-$CF_3CCl{=}CHCl$/*cis*-$CF_3CCl{=}CHCl$ had to be measured by GC-MS. These data, as well as the ratio of *trans*-$CF_3CF{=}CHCl$/*cis*-$CF_3CF{=}CHCl$, are shown in Figure 2. The ratio of 6.1 ± 0.5 for $CF_3CCl{=}CHCl$ gives a rate constant for *cis*-$CF_3CCl{=}CHCl$ of $(0.042 \pm 0.014) \times 10^{-3}$ Torr. The ratio of *trans*-$CF_3CCl{=}CHCl$/*trans*-$CF_3CF{=}CHCl$ also was measured by GC−MS as 0.17 ± 0.03, which agrees with the GC-FID measured rate constant ratio of 0.17. The GC−MS measured *trans*-/*cis*-$CF_3CF{=}CHCl$ ratio of 3.5 ± 0.5 also agrees with the 3.3 value from the rate constant ratio. These two comparisons essentially confirm the calibration of the response factors.

According to the DFT calculations, 2,3-ClF interchange has a lower threshold energy than 1,2-FCl interchange for $CF_3CFClCH_2Cl$; thus we will use the absence of a measurable yield of $CF_3CCl_2CH_2F$ or $CF_3CCl{=}CHF$ to set a limit for the k(2,3-ClF) rate constant. The retention times of $CF_3CCl_2CH_2F$ and its decomposition product, $CF_3CCl{=}CHF$, had been established in other experiments, so this was a realistic search. The *cis*-$CF_3CCl{=}CHCl$ product from reaction 2 could be observed by mass spectrometry, and the signal-to-noise ratio was such

TABLE 2: Experimental Rate Constants for $CF_3CFClCH_2Cl$ and $CF_3CFClCH_3$[a]

	Torr	s^{-1}
	$CF_3CFClCH_2Cl$[b]($\langle E\rangle = 87$ kcal mol^{-1})	
$CF_3CF{=}CHCl$ (*trans*) + HCl	0.00146 ± 0.00008	$(1.9 \pm 0.6) \times 10^4$
$CF_3CF{=}CHCl$ (*cis*) + HCl	0.00044 ± 0.00003	$(0.57 \pm 0.17) \times 10^4$
$CF_3CCl{=}CHCl$ (*trans*) + HF	0.000254 ± 0.000014	$(0.33 \pm 0.10) \times 10^4$
$CF_3CCl{=}CHCl$ (*cis*) + HF	0.000042 ± 0.000013	$(0.054 \pm 0.02) \times 10^4$
$CF_3CCl_2CH_2F$	not observed[c]	$\leq 0.03 \times 10^4$
	$CF_3CFClCH_3$[d] ($\langle E\rangle = 94$ kcal mol^{-1})	
$CF_3CF{=}CH_2$+HCl	0.367 ± 0.013	$(4.74 \pm 0.28) \times 10^6$
$CF_3CCl{=}CH_2$ + HF	0.0436 ± 0.0015	$(0.56 \pm 0.03) \times 10^6$

[a] The conversion from units of Torr to s^{-1} was done as specified in footnote a of ref 10. The larger (but not exactly known) cross sections of $CF_3CFClCH_2Cl$ are effectively balanced by the heavier reduced mass, relative to $CF_3CFClCH_3$ and we decided to use the same conversion factor of 1.30×10^7 s^{-1}/Torr as for the $CF_3CFClCH_3$ system. [b] This work; *trans* denotes that the F and Cl atoms or Cl and Cl atom have *trans*-geometry. [c] The rate constant for 2,3-ClF interchange was set as ≤ 0.5 of the rate constant for *cis*-$CF_3CCl{=}CHCl$. [d] Taken from ref 10.

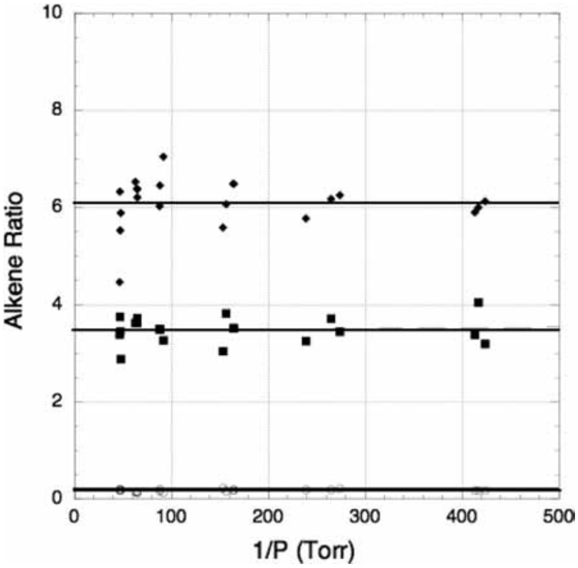

Figure 2. Plots of product ratios vs pressure^{-1}: (◆) *trans/cis*-$CF_3CCl{=}CHCl$; (■) *trans/cis*-$CF_3CF{=}CHCl$; (○) *trans*-$CF_3CCl{=}CHCl$/*trans*-$CF_3CF{=}CHCl$. The average ratios are 6.1 ± 0.5, 3.5 ± 0.5 and 0.17 ± 0.03; these data are from GC/MS measurements.

that a $CF_3CCl{=}CHF$ yield one-half of the *cis*-$CF_3CCl{=}CHCl$ yield could have been measured. Thus, we will set an upper limit of 0.03×10^4 s^{-1} as the rate constant for 2,3-ClF interchange.

The results of $CF_3CFClCH_2Cl$ are compared to those for $CF_3CFClCH_3$ in Table 2; the rate constants for $CF_3CFClCH_3$ clearly are much larger than for $CF_3CFClCH_2Cl$, with overall ratios for 2,3-ClH and 2,3-FH elimination of 193 and 150, respectively. However, the ratios of overall HCl to HF elimination are similar, 6.6 and 8.4 for $CF_3CFClCH_2Cl$ and $CF_3CFClCH_3$, respectively, even though the products for $CF_3CFClCH_2Cl$ are divided between *cis*- and *trans*-isomers. The objective of section IV.C will be to understand why the rate constants for $CF_3CFClCH_2Cl$ are so much smaller than for $CF_3CFClCH_3$. To compare experimental rate constants to calculated rate constants based on transition state models, the rate constants in Torr units must be changed to s^{-1} using the collision constant, k_M. Because the collision diameters and ϵ/k values for $CF_3CFClCH_2Cl$ with CF_3CFClI and CH_2ICl are not established and because they will be similar to those for $CF_3CFClCH_2Cl$ with CF_3FClI and CH_3I, we used the same conversion factor as for the $CF_3CFClCH_3$ system.[10] The error limits for rate constants in Table 2 are ±30%, reflecting the uncertainty associated with converting from Torr to s^{-1} units.

IV. Computational Results

IV. A. Computational Methods. The DFT calculations of energies and structures of the molecules and their transition states were done with the Gaussian-03 suite of codes.[14] The methods used to identify and characterize the transition state geometries were described in earlier publications. The $CF_3CFClCH_2Cl$ system is more complex than the $CF_3CFClCH_3$ example,[10] because of the three conformers of the $CF_3CFClCH_2Cl$ molecule and the *cis*- and *trans*-geometries of the HF and HCl elimination transition states. Most calculations were done with the B3PW91/6-31G(d′,p′) method. In some cases the energies were verified by calculations with the 6-311+G(2d,p) basis set. The $CF_3CFClCH_2Cl$ molecule has three conformers associated with internal rotation of the $-CH_2Cl$ group. The lowest energy conformer has the CF_3 group and Cl atom in the *trans*-position; however, the conformer with the two Cl atoms in the *trans*-position is only 0.05 kcal mol^{-1} higher in energy and the third conformer with Cl and F atoms in the *trans*-position is 0.60 kcal mol^{-1} above the lowest energy conformer. The barriers to internal rotation were calculated to be 4.0, 5.2 and 6.2 kcal mol^{-1}. The HCl and HF elimination transition states have *cis*- and *trans*- isomers, but only a single conformer exists for each. The 2,3-FCl interchange transition state has one conformer. The calculated harmonic vibrational frequencies, unscaled, and the three overall rotational moments of inertia were employed to obtain the statistical RRKM rate constants. The geometric mean of the frequencies of the three conformers of the molecule were used to find the density of states. In these rate constant calculations, the CF_3 and CH_2Cl torsional motions were treated as hindered internal rotors using the Multiwell code of Barker[14] to calculate sums and densities of states. Additional details about the calculations are supplied in the following sections and in the Supporting Information.

IV. B. Thermochemistry. To obtain the average energy of $CF_3CFClCH_2Cl$ molecules, the enthalpy of formation of $CF_3CFClCH_2Cl$, CF_3CFCl and CH_2Cl are needed to obtain $D_0(CF_3CFCl{-}CH_2Cl)$ for use in eq 6.

$$\langle E\rangle = D_0(CF_3CFCl{-}CH_2Cl) + 3RT + \langle E_v(CH_2Cl)\rangle + \langle E_v(CF_3CFCl)\rangle \quad (6)$$

The last two terms are the thermal vibrational energies of the radicals. The $\Delta H^0_{f,298}$ values for CH_2Cl[15] and CF_3CFCl[10] are +28.0 and −174.0 kcal mol^{-1}, respectively, but $\Delta H^0_{f,298}(CF_3CFClCH_2Cl)$ must be estimated. We used the five isodesmic reactions that are shown in Table 3. Both 6-31G(d′,p′) and 6-311+G(2d,p) basis sets were used to obtain the net changes in energy (or ΔH^0_0) for the reactions; the most stable conformer geometries were used. The difference between the

TABLE 3: Isodesmic Reaction Used to Estimate $\Delta H^0_{f,298}(CF_3CFClCH_2Cl)$

	(a) $CF_3CFClCH_3$	+	CH_3Cl	→	CH_4	+	$CF_3CFClCH_2Cl$	ΔH^0_{RX}
total energy[a]	−612053.6		−313754.5		−25390.5		−900414.4	3.2[a]
total energy[b]	−612184.0		−313779.5		−25397.2		−900563.1	3.2[b]
$\Delta H^0_{f,298}$	−229.8		−19.6		−17.8		(−228.4)[a] (−228.4)[b]	

	(b) $CF_3CFClCH_3$	+	CH_3CH_2Cl	→	C_2H_6	+	$CF_3CFClCH_2Cl$	ΔH^0_{RX}
total energy[a]	−612053.6		−338400.9		−50032.8		−900414.4	7.3[a]
total energy[b]	−612184.0		−338431.5		−50044.8		−900563.1	7.6[b]
$\Delta H^0_{f,298}$	−229.8		−26.8		−20.0		(−229.3)[a] (−229.0)[b]	

	(c) CF_3CHFCH_3	+	CH_2ClCH_2Cl	→	C_2H_6	+	$CF_3CFClCH_2Cl$	ΔH^0_{RX}
total energy[a]	−323686.3		−626767.4		−50032.8		−900414.4	6.5[a]
total energy[b]	−323799.4		−626816.6		−50044.8		−900563.1	8.1[b]
$\Delta H^0_{f,298}$	−225.6		−31.6		−20.0		(−230.7)[a] (−229.1)[b]	

	(d) CF_3CHFCl	+	CH_3CH_2Cl	→	CH_4	+	$CF_3CFClCH_2Cl$	ΔH^0_{RX}
total energy[a]	−587401.9		−338400.9		−25390.5		−900414.4	−2.1[a]
total energy[b]	−587528.0		−338431.5		−25397.2		−900563.1	−0.8[b]
$\Delta H^0_{f,298}$	−221.2		−26.8		−17.8		(−232.3)[a] (−231.0)[b]	

	(e) CF_2ClCF_2Cl	+	C_2H_6	→	CH_4	+	$CF_3CFClCH_2Cl$	ΔH^0_{RX}
total energy[a]	−875763.1		−50032.8		−25390.5		−900414.4	−9.0[a]
total energy[b]	−875907.4		−50044.8		−25397.2		−900563.1	−8.1[b]
$\Delta H^0_{f,298}$	−215.2		−20.0		−17.8		(−226.4)[a] (−225.5)[b]	

[a] Calculated total electronic energy plus zero-point energy from B3PW91/6-31G(d′,p′). [b] Calculated total electronic energy plus zero-point energy from B3PW91/6-311+G(2d,p). All entries are in kcal mol^{-1}.

ΔH^0_0 values for the two basis sets were ≤2 kcal mol^{-1} for each reaction. Combining these results with experimental $\Delta H^0_{f,298}$ for other components[16–19] gives $\Delta H^0_{f,298}(CF_3CFClCH_2Cl)$ that ranged from −225.5 to −232.3 kcal mol^{-1}. The "experimental" enthalpies of formation of the first component of reactions a−e need to be qualified. Although the overall agreement among the five reactions is good, the $\Delta H^0_{f,298}(CF_3CFClCH_3)$ and $\Delta H^0_{f,298}(CF_3CFHCH_3)$ were taken from our previous[10] set of isodesmic calculations. Fortunately, this value for CF_3CFHCH_3agrees with the calculations of Khursan.[17] The $\Delta H^0_{f,298}$ (CF_2ClCF_2Cl) is an experimentally based number, but the reliability is somewhat uncertain.[5] The global averages for ΔH^0_{RX} are −229.4 and −228.6 kcal mol^{-1} for the 6-31 G(d′,p′) and 6-311+G(2d,p) basis sets, respectively from the five reactions. We will give slightly higher weight to the first four reactions and use $\Delta H^0_{f,298}(CF_3CFClCH_2Cl) = -230 \pm 3$ kcal mol^{-1}, which corresponds to $D_{298}(CF_3CFCl{-}CH_2Cl) = 84$ kcal mol^{-1}. This value can be compared to $D_{298}(CF_3CFCl{-}CH_3) = 90.8$ kcal mol^{-1}. These bond dissociation energies have ±2−3 kcal mol^{-1} uncertainty, but the trend for $D(CF_3CFCl{-}CH_2Cl) < D(CF_3CFCl{-}CH_3)$ must be correct. Converting $D_{298}(CH_2Cl{-}CFClCF_3)$ to 0 K and adding the thermal energies gives $\langle E(CF_3CFClCH_2Cl)\rangle = 87$ kcal mol^{-1} from eq 6.

The enthalpy changes for interconversion of the four isomers below are of interest because of the possibilities for 1,2- and 2,3-FCl interchange in $CF_3CFClCH_2Cl$, which is the focus of this research. The calculated enthalpy changes based on the 6-31G(d′,p′) basis set for this sequence of reactions are (−3.8), (5.6) and (8.8) kcal mol^{-1} for lowest energy conformers.

$$CF_2ClCF_2CH_2Cl \rightarrow CF_3CFClCH_2Cl \rightarrow CF_3CCl_2CH_2F \rightarrow CF_2ClCFClCH_2F \quad (7)$$

The enthalpy change for a 2,3-ClF interchange as a fourth step, which would complete the cycle, is (−10.6) kcal mol^{-1}. The $CF_3CFClCH_2Cl$ isomer is the most stable and $CF_2ClCFClCH_2F$ is the least stable of the isomers. The endothermic nature of 2,3-FCl (5.6 kcal mol^{-1}) and 1,2-ClF (3.8 kcal mol^{-1}) interchange elevates the threshold energies and explains why interchange was *not* observed in competition with HCl or HF elimination from $CF_3CFClCH_2Cl$. The exothermic nature of 1,2-ClF interchange to convert a CF_2Cl group to a CF_3 group, with an associated low threshold energy, explains why this interchange has been observed and characterized for $CF_2ClCF_2CH_3$, $CF_2ClCHFCH_3$ and $CF_2ClCHFC_2H_5$.[1–4] In fact, experimental studies of the first and fourth members of the series in eq 7, which will be presented in the future, also exhibit exothermic ClF interchange in competition with HCl and HF elimination.[20]

IV. C. Rate Constants and Threshold Energies. RRKM rate constants were calculated for a range of E_0 values, according to eq 8 for 2,3-ClH and 2,3-FH elimination plus 2,3-FCl interchange. Although interchange was not experimentally observed, we wanted to set an experimentally based lower limit to E_0(2,3-FCl) for comparison with the DFT calculated value, which was calculated to be 1.9 kcal mol^{-1} lower than the E_0(1,2-FCl). Separate transition states were evaluated for the *trans*- and *cis*-pathways for HCl and HF elimination.

$$k_E = (s^\dagger/h)(I^\dagger/I)^{1/2} \sum P^\dagger(E - E_0)/N_E^* \quad (8)$$

All terms in eq 8 are known or can be calculated from the models, except for E_0, which was selected by comparison of k_E with the experimental result for $k\langle E\rangle$. The reaction path degeneracy, $s^\dagger$, is unity for ClF interchange and for HCl and HF elimination, because the *cis*- and *trans*-transition states are

TABLE 4: Comparison of Calculated and Experimental Rate Constants and the Threshold Energies for $CF_3CFClCH_2Cl$ and $CF_3CFClCH_3$

	rate constant (s^{-1})			
molecule		experimental	calculated	threshold energy[a] (kcal mol^{-1})
$CF_3CFClCH_2Cl$	k_{ClH} (*trans*)	1.9×10^4	1.8×10^4	62 (56.4)
$\langle E \rangle = 87$ kcal mol^{-1}	k_{ClH} (*cis*)	0.57×10^4	0.53×10^4	64 (58.9)
	k_{FH} (*trans*)	0.33×10^4	0.38×10^4	63 (63.5)
	k_{FH} (*cis*)	0.54×10^3	0.62×10^3	66 (66.3)
	k_{ClF}	$<0.3 \times 10^3$	0.23×10^3	≥ 67 (68.1)
$CF_3CFClCH_3$	k_{ClH}	4.7×10^6	4.8×10^6	58.5 (55.0)
$\langle E \rangle = 94$ kcal mol^{-1}	k_{FH}	0.56×10^6	0.52×10^6	61.3 (64.1)

[a] The values in parentheses are the DFT calculated values by the B3PW91/6-31G(d′,p′) method for both $CF_3CFClCH_2Cl$ and $CF_3CFClCH_3$.[10] A calculated threshold energy for $CF_3CFClCH_2Cl$ corresponds to the difference in energy between the lowest energy conformer of the molecule and its transition state; the experimentally assigned E_0 corresponds to an effective average for the conformer.

treated separately; the $(I^\dagger/I)$ term is the ratio of the three overall rotational moments of inertia, because the rotations are considered to be adiabatic. The sums of states, $\Sigma P^\dagger(E - E_0)$, for the transition state and the density of states, N_E^*, for the molecule were calculated[21] using hindered internal rotors to represent torsional motions of the $-CF_3$ and $-CH_2Cl$ groups. Because the $-CF_3$ torsional degree of freedom exists in both the molecule and the transition states, the description of the $-CF_3$ torsion is not very important. However, the choice of model to represent the $-CH_2Cl$ torsion is important because this motion becomes a vibration in the transition state. The difference between the $-CH_3$ and $-CH_2Cl$ groups on N_E^* will be examined in some detail to understand the reduction in rate constants for $CF_3CFClCH_2Cl$ relative to $CF_3CFClCH_3$.

The reduced moments of internal rotation, I_{red}, were calculated by the method of Pitzer and the values were $I_{red}(CF_3) = 59.4$ amu Å^2 for the molecule and 59.5, 59.6 and 70.6 amu Å^2 for the HCl, HF and ClF transition states, respectively. The $I_{red}(CH_2Cl)$ value was 79.8 amu Å^2. The potential barriers were $V(CF_3) = 4.6$ and $V(CH_2Cl) = 5.0$ kcal mol^{-1}; the same $V(CF_3)$ was used in the transition states. The $V(CH_2Cl)$ was obtained as the average of the barriers identified from the 6-31G(d′,p′) calculations.

The sums of states for the *cis*- and *trans*-transition states are very similar at the same energy. For example at $\langle E \rangle - E_0 = 25$ kcal mol^{-1}, the ratio for *cis/trans* is 1.08 for FH elimination and 1.03 for ClH elimination. However, the ClH transition state has a looser structure than the FH transition state, as previously discussed,[10] and the ratio of sums of states is 2.36 at $\langle E \rangle - E_0 = 25$ kcal mol^{-1} in favor of HCl elimination, which partially explains why HCl elimination is favored. The sums of states for the HF transition state exceeds that for ClF interchange by a factor of just 1.3.

The assigned threshold energies are summarized in Table 4 for an average energy of 87 kcal mol^{-1}. A strong correlation exists between the $\langle E \rangle$ and an assigned E_0. Because $\langle E \rangle$ has some uncertainty, several plots of k_E versus E for different E_0 are shown in Figure 3 to illustrate the range of acceptable values. The DFT calculated E_0 values are enclosed in parentheses in Table 4. The major processes, *trans*-ClH and *trans*-FH elimination, have assigned threshold energies of 62 and 63 kcal mol^{-1}, respectively. The less important channels corresponding to *cis*-elimination have 2−3 kcal mol^{-1} higher E_0 values. The larger difference in energy between the *trans*- and *cis*-geometries for FH elimination is consistent with greater steric repulsion between two Cl atoms than between a F and a Cl atom for ClH elimination. The threshold energies for *trans*-elimination from $CF_3CFClCH_2Cl$ are 4 kcal mol^{-1} higher for ClH elimination and 1.7 kcal mol^{-1} higher for FH elimination than for the corresponding processes in $CF_3CFClCH_3$.

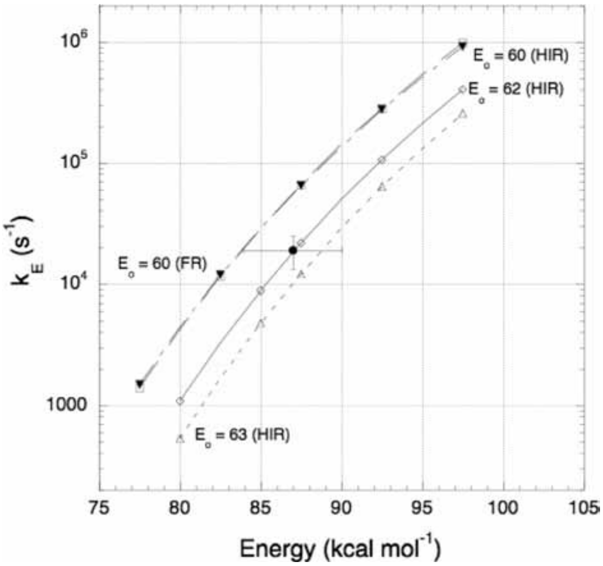

Figure 3. Plots of k_E vs E for *trans*-ClH elimination from $CF_3CFClCH_2Cl$ for three values of E_0 (all kcal mol^{-1}). The point, ●, is the experimental rate constant; the error bars give the uncertainty in k_{expt} and $\langle E \rangle$. The points shown by the filled triangles denote the rate constants for the free internal rotor (FR) model ($E_0 = 60$ kcal mol^{-1}). The three curves are for the hindered internal rotor (HIR) model with $E_0 = 60$, 62 and 63 kcal mol^{-1}. The rate constants for the FR and HIR models are nearly the same as shown for $E_0 = 60$ kcal mol^{-1}. On the scale of this plot, the k_E for *cis*-ClH elimination with the same E_0 would be the same as for *trans*-ClH.

The upper limit to the rate constant for 2,3-FCl interchange was used to give a lower limit to E_0 for this process. Although the transition state structure for interchange is somewhat tighter than the one for FH elimination, the threshold energy must still be, at least, 1−2 kcal mol^{-1} higher than for *cis*-FH elimination.

V. Discussion

Because the three barriers to internal rotation of the CH_2Cl group are similar, the symmetric hindered-rotor approximation should be satisfactory for the CH_2Cl torsion. The calculated k_E is not very sensitive to the barrier heights of the internal rotors as shown by the equivalence, which is somewhat fortuitous, of the free rotor and hindered rotor result in Figure 3. Thus, the sums and densities of states used in the RRKM calculation of k_E should have their normal reliability.[1−5,8−11] The interdependence of $\langle E \rangle$ and the assigned E_0 is illustrated for *trans*-ClH elimination in Figure 3. The ±3 kcal mol^{-1} uncertainity in $\langle E \rangle$ is more serious than the uncertainty in the experimental rate constant. Any k_E curve that passes through the rectangle defined by the error bars illustrated in Figure 3 is acceptable, in principle, and the E_0 values have ±2 kcal mol^{-1} reliability. Nevertheless, the assigned E_0 values are sufficiently reliable to establish that the threshold energies for ClH and FH elimination from $CF_3CFClCH_2Cl$ are higher than for $CF_3CFClCH_3$. The DFT calculated value for E_0(FH) was 63.5 kcal mol^{-1}, which matches the experimental result. The calculated E_0(ClH) was 56.4 kcal mol^{-1}, which is considerably lower than the experimental result of 62 kcal mol^{-1}. The DFT calculations seem to underestimate the difference in threshold energies for $CF_3CFClCH_2Cl$ versus $CF_3CFClCH_3$.

The electronic structure calculations showed that 2,3-FCl interchange had a 1.9 kcal mol^{-1} lower threshold energy than 1,2-FCl interchange. Our estimate for the lower limit to E_0(2,3-FCl) is 67 kcal mol^{-1}, which is similar to the DFT calculated value of 68.1 kcal mol^{-1}. Although ClF interchange does not compete with HCl and HF elimination for $CF_3CFClCH_2Cl$, it can be observed for other isomers of $C_3F_4Cl_2H_2$, especially $CF_2ClCFClCH_2F$.[20]

Three factors are responsible for the reduction in rate constants for $CF_3CFClCH_2Cl$ versus $CF_3CFClCH_3$: (i) The effect on N_E* of changing the CH_3 group to a CH_2Cl group, (ii) the reduction in $\langle E \rangle$ from 94 to 87 kcal mol^{-1}, and (iii) the increase in threshold energies for $CF_3CFClCH_2Cl$. The first factor can be examined by comparing rate constants for ClH elimination at the same $\langle E \rangle$, 90 kcal mol^{-1}, and the same E_0, 60 kcal mol^{-1}, with inclusion of both *cis*- and *trans*-transition states (for the same E_0) for $CF_3CFClCH_2Cl$. The ratio of rate constants is 3.4, because the density of states in eq 8 is enhanced by the CH_2Cl group. The 7 kcal mol^{-1} reduced energy contributes a factor 7.3, and the 3.5 kcal mol^{-1} change in E_0 adds a factor of 6.5. The combined result is a factor of 161. A more detailed comparison would require allowance for the different E_0 values of the *trans*- and *cis*-transition states of $CF_3CFClCH_2Cl$. This analysis suggests that the experimental rate constants, although difficult to measure, are reliable and that the small rate constants have a rational explanation.

What is responsible for the higher E_0 values and the reduced $D(CH_2Cl\text{-}CFClCH_3)$ relative to $CF_3CFClCH_3$? One clue is the difference in threshold energies for *cis*- and *trans*-configurations at the transition state for HCl and HF elimination; a similar result was found for 2,3-FH elimination from $CF_2ClCHFCH_2CH_3$.[2] The preference for the formation of products with *trans*-geometry was associated with steric repulsion energy in the olefinic-like transition state.[2] A similar explanation of the preference for *trans*-$CF_3CF{=}CHCl$ and *trans*-$CF_3CCl{=}CHCl$ from $CF_3CFClCH_2Cl$ seems probable. This repulsion energy, even for the *trans*-geometry, may increase the E_0 values for ClH and FH elimination from $CF_3CFClCH_2Cl$. Next consider the question of the bond dissociation energies. The Cl-atom repulsion energy[22] for the eclipsed configuration of CH_2ClCH_2Cl is ≈10 kcal mol^{-1}. However, the three barriers for internal rotation of the CH_2Cl group in $CF_3CFClCH_2Cl$ were similar with an average of 5 kcal mol^{-1}; the three conformers also have the same energy. Both observations suggest that the repulsive energies of the Cl atom in the CH_2Cl group interacting with the CF_3 group, the F-atom, or the Cl-atom of the CF_3CFCl group were similar. We suggest that repulsion between the Cl atom and the CF_3CFCl group is mainly responsible for the 5−6 kcal mol^{-1} reduced bond dissociation energy of $CF_3CFClCH_2Cl$ versus $CF_3CFClCH_3$. A reviewer suggested that the stabilization energy of the Cl atom in the CH_2Cl radical versus a CH_3 group may play a role in the reduced bond dissociation energy.[23] However, $D(CH_3{-}CH_2Cl)$ is only 1 kcal mol^{-1} lower than $D(CH_3{-}CH_3)$ and this seems not to be the main difference between $D(CH_2Cl{-}CFClCF_3)$ and $D(CH_3{-}CFClCH_3)$.

VI. Conclusions

Vibrationally excited $CF_3CFClCH_2Cl$ molecules were generated by the recombination of CH_2Cl and CF_3CFCl radicals in a bath gas at room temperature. Several isodesmic reactions were investigated with DFT calculations by the B3PW91/6-31G(d′,p′) and B3PW91/6-311+G(2d,p) methods to evaluate the enthalpy of formation of $CF_3CFClCH_2Cl$. The value adopted was $\Delta H^0_{f,298}(CF_3CFClCH_2Cl) = -230 \pm 3$ kcal mol^{-1}, which corresponds to $D_{298}(CF_3CFCl{-}CH_2Cl) = 84$ kcal mol^{-1}, which is 7 kcal mol^{-1} lower than $D_{298}(CF_3CFCl\text{-}CH_3)$. This thermochemistry gives $\langle E(CF_3CFClCH_2Cl) \rangle = 87$ kcal mol^{-1}.

Low pressures in large photolysis vessels were required to measure the small rate constants. The observed unimolecular reactions of $CF_3CFClCH_2Cl$ are 2,3-ClH and 2,3-FH elimination to give *cis*- and *trans*-$CF_3CF{=}CHCl$ and *cis*- and *trans*-$CF_3CCl{=}CHCl$. The *cis*- and *trans*-isomers correspond to *Z*- and *E*-geometries, respectively, with respect to the two Cl atoms in $CF_3CCl{=}CHCl$ or the F and Cl atoms in $CF_3CF{=}CHCl$. The *trans*-product is always favored, which is explained by steric repulsion energy in the transition states, which have olefinic structures for the carbon atoms in the four-centered ring. These experimental rate constants were matched with calculated RRKM rate constants based upon models from DFT calculations (B3PW91/6-31G(d′,p′)). The assigned threshold energies for the *trans*-channels for 2,3-ClH and 2,3-FH elimination are 62 and 63 kcal mol^{-1}, respectively. The threshold energies for the *cis*-channels are 2−3 kcal mol^{-1} higher. The threshold energies for $CF_3CFClCH_2Cl$ are ≈3 kcal mol^{-1} higher than for $CF_3CFClCH_3$. The 2,3-FCl interchange reaction was not observed, which suggests a 3−4 kcal mol^{-1} higher threshold energy than for *trans*-FH elimination. Other isomers of $C_3F_4Cl_2H_2$ with more favorable thermochemistry for isomerization do exhibit ClF interchange in competition with HCl and HF elimination.[20] The factors responsible for the smaller rate constants for $CF_3CFClCH_2Cl$ versus $CF_3CFClCH_3$ are the lower $\langle E \rangle$, the effect of changing the CH_3 internal rotation to a CH_2Cl internal rotation, and higher threshold energies, especially for HCl elimination.

Acknowledgment. Financial support was provided by the National Science Foundation under Grant CHE-0647582.

Supporting Information Available: Table S1 lists the calculated vibrational frequencies and moments of inertia for each conformer of $CF_3CFClCH_2Cl$ and the geometric mean used in the rate constant calculations. The computed structure for each conformer is shown. Table S2 shows the calculated vibrational frequencies and moments of inertia for each FH and ClH elimination transition state of lowest energy. The computed structures for all transition states are also shown. All calculations used the DFT method B3PW91 level of theory with a 6-31G(d′,p′) basis set. This material is available free of charge via the Internet at http://pubs.acs.org.

References and Notes

(1) Beaver, M. R.; Simmons, J. G. Jr.; Heard, G.; Setser, D. W.; Holmes, B. E. *J. Phys. Chem. A* **2007**, *111*, 8445.

(2) Burgin, M. O.; Simmons, J. G. Jr.; Heard, G. L.; Setser, D. W.; Holmes, B. E. *J. Phys. Chem. A* **2007**, *111*, 2283.

(3) Heard, G. L.; Holmes, B. E. *J. Phys. Chem. A* **2001**, *105*, 1622.

(4) Burgin, M. O.; Heard, G. L.; Martell, J. M.; Holmes, B. E. *J. Phys. Chem. A* **2001**, *105*, 1615.

(5) Lisowski, C. E.; Duncan, J. R.; Heard, G. L.; Setser, D. W.; Holmes, B. E. *J. Phys. Chem. A* **2008**, *112*, 441.

(6) Beaver, M. R.; Heard, G. L.; Holmes, B. E. *Tetrahedron Lett.* **2003**, *44*, 7265.

(7) Dolbier, W. R., Jr.; Romelaeer, R.; Baker, J. M. *Tetrahedron Lett.* **2002**, *43*, 8075.

(8) Everett, W. C.; Holmes, B. E.; Heard, G. L. To be published.

(9) Ferguson, J. D.; Johnson, N. L.; Kekenes-Husker, P. M.; Everett, W. C.; Heard, G. L.; Setser, D. W.; Holmes, B. E. *J. Phys. Chem. A* **2005**, *109*, 4540. The question of the value of the threshold energy for $CF_3CH_2CH_3$ has been resolved in favor of a higher value near 68−69 kcal mol^{-1}; see ref 11.

(10) Zhu, Li.; Simmons, J. G., Jr.; Burgin, M. O.; Holmes, B. E.; Setser, D. W. *J. Phys. Chem. A* **2006**, *110*, 1506.

(11) (a) Holmes, D. A.; Holmes, B. E. *J. Phys. Chem. A* **2005**, *109*, 10726. (b) The calculated rate constant for 1,2-FH elimination listed in Table 2 for CF_3CHFCH_3 should be $2.8 \times 10^4\ s^{-1}$, and the calculated kinetic-isotope effect for CF_3CHFCD_3 is 2.2 as quoted in the text.

(12) Roach, M. S., Sibilia, B. M.; Holmes, B. E. *J. Phys. Chem A*, to be submitted.

(13) Simmons, J. G., Jr.; Setser, D. W.; Holmes, B. E. *J. Phys. Chem A*, To be submitted.

(14) Frisch, M. J.; Trucks, G. W.; Schlegel, H. B.; Scuseria, G. E.; Robb, M. A.; Cheeseman, J. R.; Montgomery, J. A., Jr.; Vreven, T.; Kuden, K. N.; Burant, J. C.; Millam, J. M.; Iyengar, S. S.; Tomasi, J.; Barone, V.; Mennucci, B.; Cossi, M.; Scalmani, G.; Bega, N.; Petersson, G. A.; Nakatsuji, H.; Hada, M.; Ehara, M.; Toyota, K.; Fukuda, R.; Hasegawa, J.; Ishida, M.; Nakajima, T.; Honda, Y.; Kitao, O.; Adamo, C.; Jaramillo, J.; Gomperts, R.; Stratman, R. E.; Yazyev, O.; Austen, A. J.; Cammi, R.; Pomelli, C.; Ochterski, J. W.; Ayala, P. Y.; Morokuma, K.; Voth, G. A.; Salvador, P.; Dannenberg, J. J.; Zakrzewksi, V. G.; Dapprich, S.; Daniels, A. D.; Strain, M. C.; Farkas, O.; Malik, D. K.; Rabuck, A. D.; Raghavachari, K.; Foresman, J. B.; Ortiz, J. V.; Cui, Q.; Baboul, A. G.; Clifford, S.; Cioslowski, J.; Stefanov, B. B.; Liu, G.; Liashenko, A.; Piskorz, P.; Komaromi, I.; Martin, R. L.; Fox, D. J.; Keith, T. Al-Laham, M. A.; Peng, C. Y.; Nanayakkara, A.; Challacombe, M.; Gill, P. M. W.; Johnson, B.; Chen, W.; Wong, M. W.; Gonzalez, C. and Pople, J. A. *Gaussian 03*, revision B.04; Gaussian, Inc., Pittsburg, PA,2003.

(15) Seetula, J. A. *J. Chem. Soc., Faraday Trans.* **1996**, *92*, 3069.

(16) Manion, J. A. *J. Phys. Chem. Ref. Data* **2002**, *31*, 123.

(17) Khurson, S. L. *Russ. J. Phys. Chem. Suppl. 1* **2004**, *78*, S34.

(18) Yamada, T.; Fang, T. D.; Taylor, P. H.; Berry, R. J. *J. Phys. Chem. A* **2000**, *104*, 5013.

(19) (a) Buckley, G. S.; Rodgers, A. S. *J. Phys. Chem.* **1983**, *87*, 126. (b) Lacher, J. R.; McKinney, J. J.; Snow, C. M.; Michel, L.; Nelson, G.; Park, J. D. *J. Am. Chem. Soc.* **1949**, *71*, 1330.

(20) Zaluzhna, O.; Simmons, J. G., Jr.; Setser, D. W.; Holmes, B. E. *J. Phys. Chem. A.* **2008.**

(21) Barker, J. R. *Int. J. Chem. Kinet.* **2001**, *33*, 232.

(22) El Youssoufi, Y.; Herman, M.; Lievin, J. *Mol. Phys.* **1998**, *87*, 461.

(23) Mayer, P. M.; Glukhovtsev, M. N.; Gauld, J. W.; Radom, L. *J. Am. Chem. Soc.* **1997**, *119*, 12889.

JP800488Q